

True MRI Assessment of Stem Cell Chondrogenesis in a Tissue Engineered Matrix

Padmabharathi Pothirajan, Deborah Dorcemus, Syam Nukavarapu, and Mrignayani Kotecha*

Abstract— Developing a non-invasive method to monitor the growth of tissue-engineered cartilage is of utmost importance for tracking the progress and predicting the success or failure of tissue-engineering approaches. Magnetic Resonance Imaging (MRI) is a leading non-invasive technique suitable for follow-through in preclinical and clinical stages. As complex tissue-engineering approaches are being developed for cartilage tissue engineering, it is important to develop strategies for true non-invasive MRI monitoring that can take into account contributions of the scaffold, cells and extracellular matrix (ECM) using MR parameters. In the current study, we present the preliminary MRI assessment of chondrogenic differentiation of human bone marrow derived stem cells seeded onto a specially designed osteochondral matrix system. We performed water relaxation times (T_1 and T_2) MRI measurements at 7, 14 and 28 days after cell seeding. The MRI experiments were performed for the tissue-engineered cartilage as well as for acellular scaffolds. We identified that the contribution of the scaffold is the dominant contribution in MR parameters of engineered cartilage and that it hinders observation of the tissue growth. An attempt is made to filter out this contribution, for the first time, in order to make a true observation of tissue growth using MRI.

I. INTRODUCTION

Cartilage and osteochondral tissue engineering have been an active field of research for the past two decades and a variety of tissue-engineering approaches are being investigated. In order to mimic native tissue in the laboratory, tissue engineers use a variety of strategies involving scaffolds (natural and synthetic), cell sources (Chondrocytes or Mesenchymal stem cells), and cell culture conditions (biophysical and biochemical cues) [1]. An ideal scaffold should be mechanically stable and biologically capable of promoting cell adhesion, proliferation and differentiation. The adult human body has a limited source of chondrocytes, therefore, multi-potent stem cells capable of chondrogenic lineage are an attractive and practical choice for cartilage and osteochondral tissue engineering [2]. Since the production of extracellular matrix (ECM)

components is the main criteria for success, there is a strong emphasis on a fast rate of high ECM production. As a result, engineered tissues often have a different morphology when compared to native cartilage as shown in Figure 1, one that is strongly dependent on the scaffold's properties.

Currently, when evaluating tissue-engineered cartilage, the production of proteoglycans (PG) and type-II collagen are used as biomarkers for success. These ECM components are assessed by biochemical techniques that include quantitative glycosaminoglycan (GAG) and collagen assays, gene expression analyses using quantitative real-time polymerase chain reaction (qRT-PCR) and histological staining [3-7]. When scaffolds are implanted in animals, they are removed at different time points and analyzed *ex vivo*. Unfortunately, most current characterization methods, including immunohistochemistry and biochemical analysis are destructive and do not have the potential to map the tissue morphology. Yet, tissue morphology defines the tissue functionality.

Our group has been working on the early stage non-invasive magnetic resonance spectroscopy (MRS) and imaging (MRI) characterization of tissue-engineered cartilage for several years [1, 8-11] and we found that challenges in this area are many fold. From a technological standpoint, the challenge lies in the unambiguous quantification of ECM growth using MRS/MRI in the presence of a scaffold and cells. From the point view of assisting tissue engineers, the challenge lies in standardization of MR techniques that tissue-engineers can

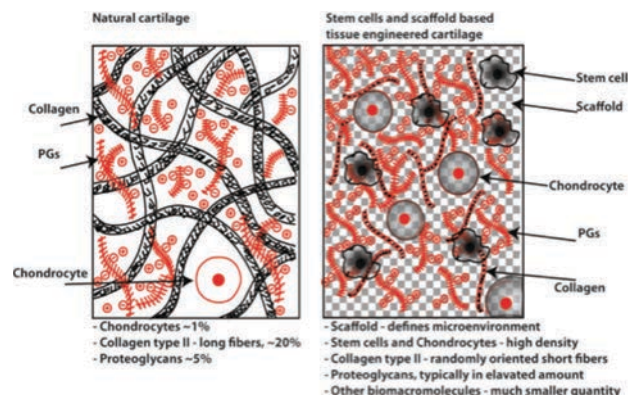


Figure 1: Schematic diagram showing differences between the morphology of native and engineered-cartilage tissues. Native cartilage has a smaller number of cells and 4 times more collagen than proteoglycans. The collagen fibers are long and oriented along the depth of the tissues. In comparison, in engineered tissues, very often cells are seeded in high density to ensure high ECM production. Commonly the amount of proteoglycan is elevated and collagen fibers may be short and of random orientation.

Research was partially supported by NIH/NIBIB EB007537, AO foundation (S-13-122N), Department of Defense (W81XWH-11-1-0262) and NSF Bridge to Doctorate program (award number 124983).

M. Kotecha is with the Department of Bioengineering, University of Illinois at Chicago, Chicago, IL 60615, USA (phone: 312-413-2018; fax: 312-996-5921; e-mail: mkotecha@uic.edu).

P. Pothirajan is with the Department of Bioengineering, University of Illinois at Chicago, Chicago, IL 60615, USA (email: ppothi2@uic.edu).

D. Dorcemus is with the Institute for Regenerative Engineering and the Department of Biomedical Engineering, University of Connecticut Storrs, CT 06269, USA (email: deborah.dorcemus@uconn.edu).

S. Nukavarapu is with the Institute for Regenerative Engineering, Biomedical Engineering, Material Science and Engineering, Department of Orthopedic Surgery, University of Connecticut Health Center, Farmington CT 06230, USA (email: syam@uuchc.edu).

use in their routine assessments. Here we can take advantage of the unique capabilities of MR to provide information about molecular dynamics and tissue microstructure non-invasively. This complements current assessment methods of engineered tissues that might be crucial in assessing tissue functionality.

Cartilage is 70-80% water; therefore, the dynamics of water protons, gauged using its relaxation times (e.g. T_1 and T_2) and apparent diffusion coefficient (ADC), provides a window into the biomechanical properties of the tissue [1]. The typical MRI characterization of engineered cartilage relies on changes in water T_1 , T_2 and ADC with an increasing amount of PG and collagen [1, 12]. We have shown, as have other scientists, that the correlation between the change in MR parameters and the change in growing ECM holds true for chondrocyte-based tissue-engineered approaches [13-15]. However, the situation is far more dramatic when observing the chondrogenesis of stem cells seeded in scaffold-based cartilage tissue engineering using MRI. Here, the scaffold environment dominates in water proton magnetic resonance properties.

The scaffold system we used in this study is uniquely designed to best support osteochondral defect repair and regeneration. The scaffolds have a gradient porous structure composed of a biodegradable polyester, poly(85 lactide-co-15 glycolide) (PLGA) [16]. As a first step, the gradient structure is infiltrated with a peptide hydrogel containing human bone marrow stromal cells to form an advanced gradient hybrid matrix [16-18]. The matrix design is such that it has the ability to provide bone and cartilage specific growth factors in a gradient fashion. We observed chondrogenesis of stem cells in this scaffold system as a function of growth time for four weeks using MRI. The T_1 and T_2 MRI experiments were performed on 7, 14, and 28 days after cell seeding. Our long term goal in this project is to be able to identify both the cartilage and bone growth phases non-invasively using MRI.

II. MATERIALS AND METHODS

A. Preparation of Unique gradient scaffold

Stem cell differentiation is regulated by numerous cues in their microenvironment. The porous 3D tissue scaffold provides those cues and is the basis of tissue engineering [19, 20]. In tissue engineering, one of the most important factors is the design of a proper scaffold, which provides the necessary biological and mechanical environment to the encapsulated cells. In order to yield functional native-like cartilage tissues, 3D encapsulation of stem cells with hydrogels have been identified as an excellent choice. Hydrogels possessing a high water content have been used as biomaterials for tissue engineering because of their efficiency in transporting nutrients and waste products and also for their unique biocompatibility [20].

We used an advanced “Polymer-Hydrogel” scaffold with gradient properties for cartilage regeneration. An oil-in water emulsion of the poly(85 lactide-co-15 glycolide) (PLGA) polymer was used to fabricate microspheres. These PLGA microspheres were then combined with increasing NaCl porogen, to produce PLGA matrices with gradient pore

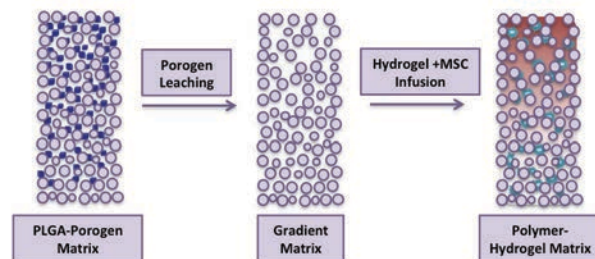


Figure 2: Schematic diagram of “Polymer-Hydrogel” scaffold fabrication

volume along the scaffold length [17, 21]. Finally, the sintered scaffold was porogen leached, leaving in its place the completed scaffold with gradient porosity increasing from bottom to top [17, 18]. In order to cellularize the scaffold bone marrow derived human mesenchymal stem cells (BM-hMSCs) were first combined with puramatrix hydrogel. These human bone marrow stromal cells (500 K/scaffold), embedded in the hydrogel, were then added to the pores of the gradient scaffold, infiltrating the pore spaces. The cell-seeded matrices were cultured in chondrogenic media (i.e., high glucose DMEM supplemented with 50 μ g/ml ascorbic acid 2-phosphate, 0.1 μ M dexamethasone, 100 μ l/ml sodium pyruvate, ITS⁺, 10ng/ml TGF- β 1, 40 μ g/ml L-proline and 1% penicillin-streptomycin) for cellular differentiation and matrix formation. Fig. 2 illustrates the schematic diagram of the scaffold fabrication process. The scaffolds were 4 mm in diameter and 8 mm in height.

B. Biochemical Analysis

Prior to biochemical analysis with the full gradient structure disk scaffolds of 10 mm diameter and 2 mm height were fabricated with 30% porogen using the same thermal sintering and porogen leaching methods previously mentioned [21]. The porous scaffolds were seeded with BM-hMSCs embedded in puramatrix hydrogel, with 450,000 cells/scaffold, and cultured in a chondrogenic media. After 21 days of culture the samples were fixed in 10% formalin, washed in phosphate buffered saline (PBS), and were fluorescently stained for the presence of type-II collagen and Sox9. Additionally, cell morphology was visualized through the staining of Tubulin. Briefly, this procedure entails permeabilization with .25% Triton x100, blocking in 10% goat serum, incubation with the primary, followed by the fluorescent secondary, with both antibodies made in 1% goat serum, and finally nuclei staining with 1mg/ml propidium iodide. Scaffolds stained with Anti-Collagen II, Anti-Sox9, or Anti-Tubulin were visualized using Zeiss LSM ConfoCor2.

Gradient scaffolds, 4 mm diameter and 8 mm height, were infiltrated with cell embedded puramatrix hydrogel (500,000 cells/scaffold), and cultured for 28 days in chondrogenic media. At 7, 14 and 28 days samples were taken out of culture, crushed, and digested for 16 hours in a proteinase K solution containing Tris/EDTA buffer, 0.185 mg/ml iodoacetamide, 0.01mg/ml pepstatin A, and 1 mg/ml proteinase K in a 56°C water bath. Portions of the digested samples were treated with dimethylmethylene blue (DMMB) as well as PicoGreen dsDNA quantitation reagent for GAG and DNA quantification, respectively. For the DMMB assay,

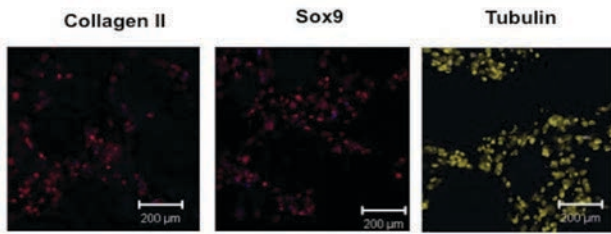


Figure 3: Immunofluorescence performed after 450,000 cells were seeded and cultured for 21 days showing positive staining for both Collagen II as well as Sox9 with Tubulin depicting typical rounded cell morphology and cellular condensation.

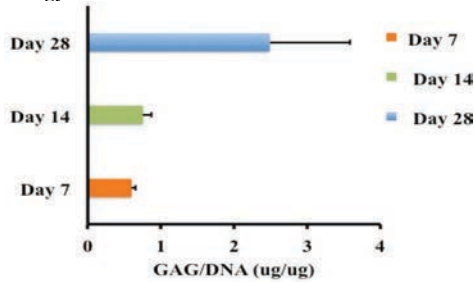


Figure 4: Quantification of GAG/DNA ratio obtained from DMMB and Picogreen assays.

absorbance was read at 520 nm and the DNA assay measures fluorescence at 485 nm/535 nm using a BioTek Synergy™ HT. The results are compared to the standards made with chondroitin sulfate and lambda DNA.

C. MRI experiments

The MRI measurements were performed using a Bruker Avance DRX 11.7 T (500 MHz) micro-imaging facility controlled by the Bruker imaging software Paravision 4.0 using a 5 mm proton RF coil. The experiments were performed in chondrogenic growth media to preserve the natural environment of engineered tissues. Figure 5 shows the schematic of the MRI measurement.

The MRI experiments were performed using the following parameters: FOV = 10 mm x 10 mm, matrix size = 128 x 128, slice thickness = 0.5 mm, in-plane resolution = 78 μm x 78 μm, number of slices = 7. The T₁ parametric map was acquired using the RAREVTR pulse sequence (RARE with variable TR) using the following parameters TE = 11.5 ms, and TR in 12 steps from 114, 303, 512, 745, 1010, 1314,

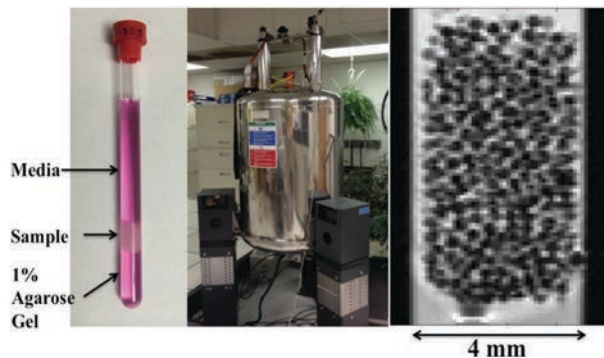


Figure 5: Schematic of MRI measurement of engineered tissues. From left to right: (A) one sample with 4 mm diameter and 8 mm height in a 5 mm tube, (B) 11.7 T Bruker microimaging system used in this study, and (c) Representative T₂-weighted image of an empty scaffold without hydrogel. The black spots are PLGA microspheres.

1674, 2112, 2675, 3460, 4772, and 5500 ms. The T₂ relaxation time measurements were measured using MSME pulse sequence (multi slice multi echo) and TE = 7.2 ms, no. of echoes = 32 and TR = 4 s. The T₂ and T₁ relaxation times were calculate using the single exponential fit. All data were processed using custom written Matlab program.

III. RESULTS

A. Chondrogenesis of Stem Cells Confirmed by Biochemical Analysis:

After 21 days immunofluorescent staining shows (Fig. 3) positive expression for type-II collagen as well as Sox9. Sox9 is an important transcriptional factor in cartilage formation that precedes and overlaps type-II collagen expression and assists in chondrocyte condensation. This cellular condensation, a morphological characteristic typical in cartilage cells can be seen in the tubulin staining also seen in Figure 3. Furthermore, biochemical analysis of the full gradient scaffold shows up regulation of the GAG content over time as a function of the overall cell number, depicted through DNA content in Figure 4.

B. MRI estimation of Tissue Matrix Growth

Figure 6 gives an illustrative example of T₁ and T₂ maps of these tissue-engineered cartilage constructs with and without cells at day 7 and day 28.

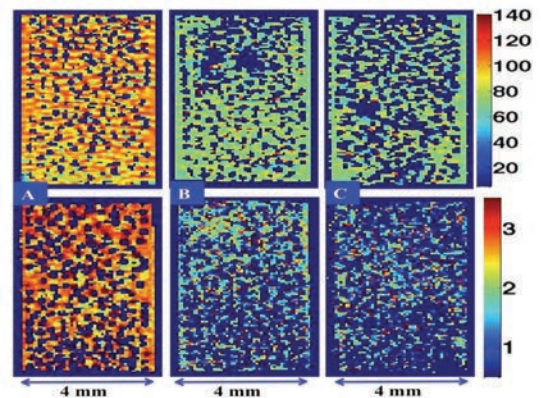


Figure 6: T₂ maps (top panel, ms) and T₁ maps (bottom panel, sec) for (A) empty scaffold (PLGA+ puramatrix hydrogel system), (B) engineered cartilage (scaffold + cells + ECM) at day 7 and (C) engineered cartilage (scaffold + cells + ECM) at day 28.

Table 1: Measured and the calculated (boxed blue in the last column) (a) T₂ (b) T₁ for tissue engineered cartilage.

Table 1 (a)	T ₂ (cells + ECM + scaffold) (n = 3) ms (± sd)	T ₂ scaffolds (n = 3) ms (± sd)	T ₂ (ECM + cells) (calculated) ms (± sd)
Day 7	79.8 (± 12.1)	98.3 (± 12.1)	417 (± 63)
Day 14	76.5 (± 10.4)	98.3 (± 12.1)	349 (± 46)
Day 28	76.3 (± 11.6)	98.3 (± 12.1)	344 (± 51)
Table 1 (b)	T ₁ (cells + ECM + scaffold) (n = 3) sec (± sd)	T ₁ scaffolds (n = 3) sec (± sd)	T ₁ (ECM+cells) (calculated) sec (± sd)
Day 7	2.6 (± 0.7)	2.8 (± 0.3)	18.5 (± 2.3)
Day 14	2.3 (± 0.9)	2.8 (± 0.3)	11.5 (± 3.6)
Day 28	2.0 (± 0.9)	2.8 (± 0.3)	5.4 (± 1.3)

Average number of voxels = 1561 ± 307

Table 1 presents the measured relaxation times in the first two columns along with calculated relaxation times for the ECM and cell contributions as boxed in blue. The scaffold system had a gradient porous matrix system. The more porous region of this matrix system is expected to support chondrogenesis of stem cells whereas the less porous region is expected to support the osteogenic differentiation. The T_1 and T_2 values for ECM and cells were calculated using the following equation:

$$R_x(\text{ECM} + \text{cells}) = R_x(\text{cells} + \text{scaffold} + \text{ECM}) - R_x(\text{scaffold})$$

where $x = 1$ or 2 , $R_1 = 1/T_1$ and $R_2 = 1/T_2$.

A few points can be noted from Fig. 6 and Table 1: (a) Because of the distribution in scaffold's pore size (100 – 500 μm), there is a significant distribution in the MRI parameters. This makes true MRI assessment a challenging task. (b) Scaffold contribution in MRI parameters is the most dominate contribution. This hinders the observation of true ECM growth using MRI if this contribution is not filtered. (c) Both aggregate T_1 and T_2 values decrease marginally as a function of tissue growth, however because of the dominant scaffold contribution, this does not represent the true tissue growth. (c) The calculated T_2 and T_1 values that are representative of true tissue growth decrease sharply as a function of time. Figure 7 shows the correlation of calculated R_1 (ECM+cells) with GAG/DNA amount.

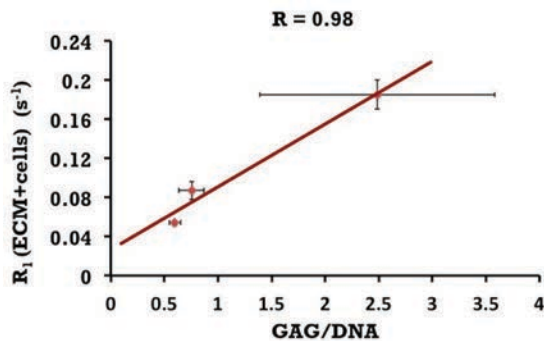


Figure 7: A strong correlation is found between the calculated relaxation rate $R_1(\text{ECM+cells}) (= 1/T_1(\text{ECM+cells}))$ and GAG/DNA amount. The red line is the trend line.

IV. CONCLUSION

In the current study, we observed the chondrogenesis of stem cells in a complex hydrogel-scaffold system using parametric MRI. We found that the scaffold contribution is the most dominate contribution in MRI parameters. A simple model was used to calculate T_2 and T_1 values associated with ECM and cells. We found that there is a strong correlation between calculated T_1 (ECM+cells) with GAG/DNA amount. This study shows that it is possible to use MRI for the growth assessment of stem cells and scaffolds based tissue-engineered cartilage.

REFERENCES

[1] M. Kotecha, D. Klatt, and R.L. Magin: "Monitoring cartilage tissue engineering using magnetic resonance spectroscopy, imaging and elastography", *Tissue Engineering Part B*, 2013, 19, (6), pp. 470-484.
 [2] R.S. Tuan, G. Boland, and R. Tuli: "Adult mesenchymal stem cells and cell-based tissue engineering", *Arthritis research & therapy*, 2003, 5, (1), pp. 32-45.

[3] B. Petit, K. Masuda, A.L. DSouza, L. Otten, D. Pietryla, D.J. Hartmann, N.P. Morris, D. Uebelhart, T.M. Schmid, and E.J.M.A. Thonar: "Characterization of crosslinked collagens synthesized by mature articular chondrocytes cultured in alginate beads: Comparison of two distinct matrix compartments", *Experimental Cell Research*, 1996, 225, (1), pp. 151-161.
 [4] S. Chandrasekhar, M.A. Esterman, and H.A. Hoffman: "Microdetermination of Proteoglycans and Glycosaminoglycans in the Presence of Guanidine-Hydrochloride", *Anal Biochem*, 1987, 161, (1), pp. 103-108.
 [5] S. Chubinskaya, K. Huch, M. Schulze, L. Otten, M.B. Aydelotte, and A.A. Cole: "Gene expression by human articular chondrocytes cultured in alginate beads", *J Histochem Cytochem*, 2001, 49, (10), pp. 1211-1219.
 [6] C.D. Hoemann: "Molecular and biochemical assays of cartilage components", *Methods Mol Med*, 2004, 101, pp. 127-156.
 [7] R. Schulz, S. Hohle, G. Zernia, M. Zscharnack, J. Schiller, A. Bader, K. Arnold, and D. Huster: "Analysis of extracellular matrix production in artificial cartilage constructs by histology, immunocytochemistry, mass spectrometry, and NMR spectroscopy", *Journal of nanoscience and nanotechnology*, 2006, 6, (8), pp. 2368-2381.
 [8] P. Pothirajan, S. Ravindran, A. George, R. Magin, and M. Kotecha: "Magnetic resonance spectroscopy and imaging can differentiate between engineered bone and engineered cartilage". IEEE-EMB, Chicago 2014.
 [9] M. Kotecha, T.M. Schmid, B. Odintsov, and R. Magin: "Reduction of water diffusion coefficient with increased engineered cartilage matrix growth observed using MRI". IEEE-EMB, Chicago 2014.
 [10] M. Kotecha, Z. Yin, and R.L. Magin: "Monitoring Tissue Engineering and Regeneration by Magnetic Resonance Imaging and Spectroscopy", *Journal of Tissue Science and Engineering*, 2013, S11:007, pp. 1-7.
 [11] M. Kotecha, S. Ravindran, T.M. Schmid, A. Vaidyanathan, A. George, and R.L. Magin: "Application of sodium triple-quantum coherence NMR spectroscopy for the study of growth dynamics in cartilage tissue engineering", *NMR in biomedicine*, 2013, 26, (6), pp. 709-717.
 [12] B. Sharma, S. Fermanian, M. Gibson, S. Unterman, D.A. Herzka, B. Cascio, J. Coburn, A.Y. Hui, N. Marcus, G.E. Gold, and J.H. Elisseeff: "Human Cartilage Repair with a Photoreactive Adhesive-Hydrogel Composite", *Science Translational Medicine*, 2013, 5, (167), pp. 167ra166.
 [13] Z. Yin, T.M. Schmid, L. Madsen, M. Kotecha, and R.L. Magin: "Monitoring the Formation of Tissue-Engineered Cartilage in Scaffold-Free Pellet Culture Using Magnetic Resonance Imaging". Proceedings of the International Society for Magnetic Resonance in Medicine (ISMRM) 20th Annual Meeting and Exhibition, Melbourne, Australia, May 4-11 2012.
 [14] S. Miyata, T. Numano, K. Homma, T. Tateishi, and T. Ushida: "Feasibility of noninvasive evaluation of biophysical properties of tissue-engineered cartilage by using quantitative MRI", *J Biomech*, 2007, 40, (13), pp. 2990-2998.
 [15] S. Miyata, K. Homma, T. Numano, T. Tateishi, and T. Ushida: "Evaluation of negative fixed-charge density in tissue-engineered cartilage by quantitative MRI and relationship with biomechanical properties", *Journal of biomechanical engineering*, 2010, 132, (7), pp. 071014.
 [16] J.C. Igwe, P.E. Mikael, and S.P. Nukavarapu: "Design, fabrication and in vitro evaluation of a novel polymer-hydrogel hybrid scaffold for bone tissue engineering", *J Tissue Eng Regen Med*, 2014, 8, (2), pp. 131-142.
 [17] D.L. Dorcemus, and S. Nukavarapu: "Novel and Unique Matrix Design for Osteochondral Tissue Engineering". 2013 MRS Fall meeting, Materials Research Society, Boston, MA, Dec 1-6 2013.
 [18] S.P. Nukavarapu, and D.L. Dorcemus: "Osteochondral tissue engineering: current strategies and challenges", *Biotechnology advances*, 2013, 31, (5), pp. 706-721.
 [19] N.S. Hwang, M.S. Kim, S. Sampattavanich, J.H. Baek, Z. Zhang, and J. Elisseeff: "Effects of three-dimensional culture and growth factors on the chondrogenic differentiation of murine embryonic stem cells", *Stem Cells*, 2006, 24, (2), pp. 284-291.
 [20] N.S. Hwang, S. Varghese, and J. Elisseeff: "Cartilage tissue engineering: Directed differentiation of embryonic stem cells in three-dimensional hydrogel culture", *Methods Mol Biol*, 2007, 407, pp. 351-373.
 [21] A.R. Amini, D.J. Adams, C.T. Laurencin, and S.P. Nukavarapu: "Optimally porous and biomechanically compatible scaffolds for large-area bone regeneration", *Tissue engineering. Part A*, 2012, 18, (13-14), pp. 1376-1388.